IEEE Trans Nucl Sci, NS-47, pp. 860-864, 2000

Measurements of the Intrinsic Rise Times of Common Inorganic Scintillators[1]

S. E. Derenzo[2], M. J. Weber[2], W. W. Moses[2], and C. Dujardin[3]

[2]Lawrence Berkeley National Laboratory, Berkeley, CA 94720 USA

[3]Laboratoire de Physico-Chimie des Matériaux Luminescents, U.R.A. C.N.R.S. No 442, Université Claude Bernard Lyon I, Villeurbannes, France

Abstract

The intrinsic rise times of a number of common inorganic scintillators are determined using ultrafast measurements of luminescence following pulsed x-ray excitation. A Ti-sapphire mode-locked laser and a light-excited x-ray tube are used to produce x-ray pulses with 60 ps fwhm. Fluorescence photons are detected with a microchannel phototube and the response of the phototube and electronics is 45 ps fwhm. Samples are either powders or thin crystals painted black on five sides to reduce delayed scattered photons. The intrinsic scintillators CeF_3, $CdWO_4$, $Bi_4Ge_3O_{12}$, and CsI have rise times $\leq$ 30 ps, indicating that electrons are promptly captured to form the excited states. The activated scintillators CaF_2:Eu, ZnO:Ga, and Lu_2SiO_5:Ce have rise times $\leq$ 40 ps, indicating that the luminescent centers are excited by rapid sequential hole capture- electron capture. The activated scintillators CsI:Tl and $YAlO_3$:Ce have slower rise times due to processes that delay the formation of excited states. It is shown that for practical scintillation detectors, internal reflections in the crystal can degrade observed rise times by hundreds of ps depending on size, reflector, and index of refraction.

I. INTRODUCTION

Scintillator rise times are of interest because they can be used to study mechanisms that affect the formation of excited states. The purpose of this work is to measure the rise times of common inorganic scintillators with sufficient accuracy to discriminate between excitation by hot charge carriers (< 10 ps) and mechanisms that are generally slower, such as the diffusion of lattice-relaxed holes, electron trapping-detrapping, and exciton diffusion.

Scintillation results from different excitation processes. In the case of core-valence luminescence (e.g., the fast component of BaF_2), holes are created in an upper core level and electrons from the valence band are immediately available to begin the emission process. The rise time of this luminescence is < 10 ps and is used in this work as a zero rise time calibration.

[1]Work supported by U.S. DOE Contract DE-AC03-76SF00098 & U.S. NIH grant R01-CA48002.

In the case of excitonic luminescence (e.g., CsI), the creation of excitons is fast, and occurs during the relaxation of the hot electrons and holes to the bottom of the conduction band and the top of the valence band, respectively.

In the case of self-activated scintillators, where the luminescent center is a major constituent (e.g., CeF_3, $Bi_4Ge_3O_{12}$, $PbWO_4$, $CdWO_4$), holes form at or near the luminescent center and then can trap mobile electrons to form excited states.

In the case of activated scintillators, carrier transport can be retarded by trapping, resulting in slow rise times. One of the goals of this work was to determine whether activated scintillators could be excited by hot carriers, which would result in fast rise times. For this purpose CsI:Tl, $YAlO_3$:Ce, CaF_2:Eu, CdS:Te, ZnO:Ga, and Lu_2SiO_5:Ce were measured.

We also show that even in small crystals, internal reflections can seriously degrade the observed rise time. To measure intrinsic fast rise times, it is necessary to use samples that are powders or thin crystals painted black on five sides.

II. EXPERIMENTAL

A. Pulsed X-Ray Source

The system (Fig. 1) consists of the following key components: (1) a diode-pumped, frequency-doubled Nd:YAG laser (Millennia model, Spectra Physics, Mountain View, CA) that produces 5 W of continuous 532-nm light, (2) a mode-locked Ti-Sapphire laser (Model 3941-M1S, Spectra Physics) that produces 1-ps pulses of 800-nm light at a frequency of 83 MHz and an average power of 1 W, (3) a pulse selector and frequency doubler (Model 3980-3S, Spectra Physics) that uses a Bragg cell to select optical pulses at a frequency up to 4 MHz and produces a primary 800-nm beam and a frequency-doubled 400-nm beam using a lithium triborate second harmonic generation crystal, (4) a light-excited x-ray tube with a multi-alkali photocathode and a tungsten anode (Model N5084, Hamamatsu, Corp., Japan), and (5) a microchannel phototube (R1564U, Hamamatsu Corp.) to detect single photons in the spectral range between 180 and 600 nm.

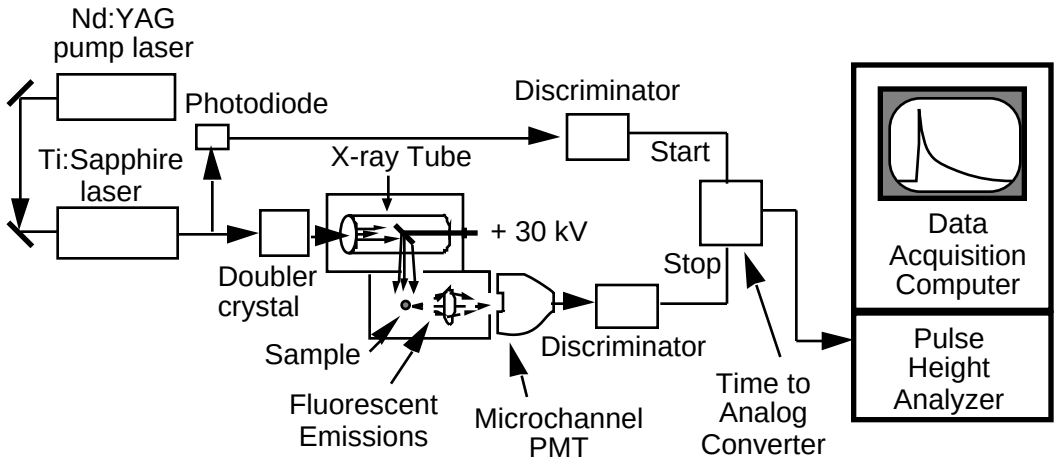

Figure 1: Pulsed x-ray source, fluorescence detection, and readout electronics.

This system was improved over the system previously described in refs. [1-3] by replacing the pulsed laser diode with components 1-3 above. The laser energy per pulse was increased from 0.01 nJ (650 nm) to 0.4 nJ (400 nm) and the number of x-rays per pulse was increased by approximately a factor of 100.

The x-ray tube was operated at +30 kV and a 0.51-mm Al window was used to filter out low energy x-rays. Under those conditions, the mean x-ray energy is 18.7 keV [3]. The attenuation length of such x-rays in BGO is 20 μm, thus bulk rather than surface effects are dominant in these studies.

B. Data Acquisition

The data acquisition electronics was designed to process signals from individual fluorescent photons and measure time spectra using the delayed coincidence method [4]. An event trigger is generated from the pulse-selected 800-nm primary laser beam by a fast photodiode (Model ET2000, Electro-Optics Technology, Inc., Traverse City. MI). A time-to-amplitude converter is started by this trigger and is stopped by individual photons detected by the microchannel tube. The converter output is sent to a pulse height analyzer consisting of a 16-bit analog-to-digital converter and a 12-bit digital-to-analog converter used to implement sliding-scale linearization [5]. The time bin width was 3.0 ps from –0.8 ns to +0.8 ns and progressively increased by powers of two for earlier and later times to reduce the number of time spectrum bins for fitting. In this way we recorded and fit data from –6 ns to +160 ns using only 1900 time bins.

The laser pulse selector rate was 80 kHz for CaF_2:Eu and $CdWO_4$ (which have long decay times) and 800 kHz for all other samples. A iris between the crystals and the microchannel phototube was adjusted as needed to reduce the detection rate to 2,000 photons/s. At this rate over 7 million time spectrum events are recorded per hour. All samples were measured at room temperature with the same experimental system and analyzed with the same methods.

C. Samples

Figure 2 shows the decay time spectra of BaF_2 for the following crystals: (1) a 10-mm cube polished and covered by white Teflon tape for high light output, (2) a 10-mm cube roughened on five sides by abrasion with 320-grit carborundum paper and coated with Kodak No. 4 dull black lacquer, and (3) a 2 x 10 x 10-mm crystal similarly roughened and coated on five sides. In all three cases the x-ray beam entered and the fluorescent photons exited from the polished uncoated 10 x 10 mm face. Figure 3 shows the decay time spectra from three similarly prepared crystals of $PbWO_4$. It is clear from these figures that intrinsic rise times can only be measured using thin crystals that have been painted black on five sides. The effect of delayed light due to scattering in the crystal with a white reflector is more substantial for $PbWO_4$, whose index of refraction (≈2.2) is higher than that of BaF_2 (1.47). Powders in fused quartz cuvettes were used only for BaF_2 and ZnO:Ga, which have a high initial intensity and whose data are not significantly affected by the fluorescence from the fused quartz.

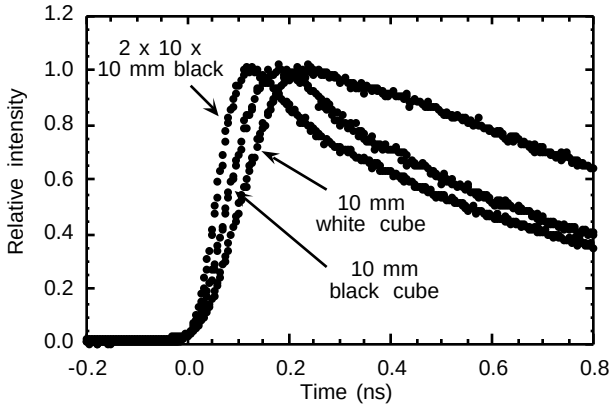

Figure 2: Normalized fluorescence time spectra from three BaF_2 crystals of different sizes and surface reflectors.

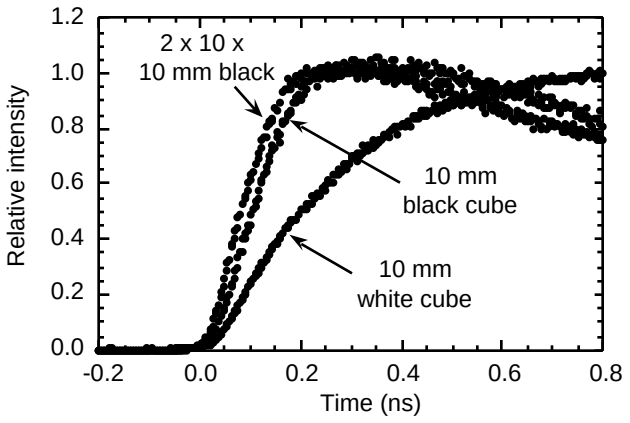

Figure 3: Normalized fluorescence time spectra from three $PbWO_4$ crystals of different sizes and surface reflectors.

D. Measurement of Impulse Response

To measure the combined time responses of (1) the microchannel phototube, (2) the fast diode trigger, (3) the time-to-amplitude converter, and (4) the pulse height analyzer, the 400-nm pulsed laser beam was heavily attenuated with optical filters and directed onto the microchannel phototube. All conditions were the same as during normal data acquisition, except that the light-excited x-ray tube and the fluorescent sample were replaced by a dense filter. The resulting time spectrum had a fwhm of 45 ps.

To simulate the response of the light-excited x-ray tube, this impulse response was then convolved with Gaussian distributions ranging from 20 ns to 100 ns fwhm. Since the response of the x-ray tube was not reliably known, data from a 2-mm thick BaF_2 crystal with five sides painted black were acquired and the best fit rise time was plotted as a function of the Gaussian width (Fig. 4). Assuming < 1 ps rise time for this core-valence emission, we conclude that the response of the x-ray tube is 60 ps fwhm and use the resulting overall impulse response for all subsequent fits.

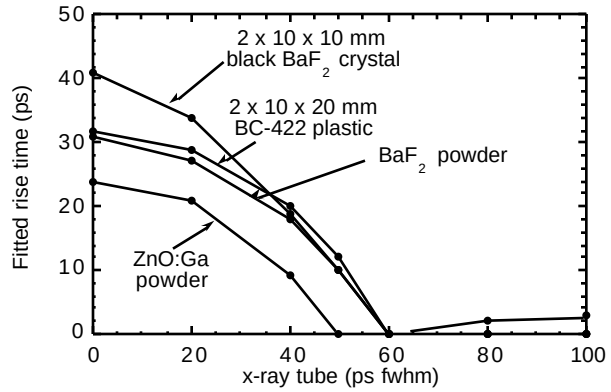

Figure 4: Fitted rise time vs. fwhm of Gaussian used to simulate the time response of the x-ray tube.

As shown in Fig. 4, the same behavior was observed for BaF_2 powder and for a 2 mm piece of BC-422 plastic scintillator painted black on five sides. The rise time of BC-422 was previously measured to be < 20 ps [6]. A powdered sample of ZnO:Ga from the early Westinghouse work [7] exhibited a slightly faster rise time, which indicates that the x-ray tube response could be as low as 50 ps fwhm and that delayed photons from light scattering could have affected the data from the other samples to a small extent.

III. Data Analysis

To determine the rise and decay times, a sum of rise and decay components was convolved with the impulse response of the system and the luminescent parameters varied to obtain a best chi-squared fit to each observed scintillation time spectrum. As described in the previous section, the system impulse response $G(t)$ was determined as the convolution of (1) the response when the heavily filtered 400-nm pulsed beam was sent directly to the microchannel tube and (2) a Gaussian distribution with 60 ps fwhm. The fitting program convolves a sum of exponential components with the impulse response function and varies the fractions f_j, rise times τ_{rj}, and decay times τ_{dj} of each component as well as an overall time shift t_0 and a time-independent background intensity B to minimize χ^2. The intrinsic fluorescence decay intensity I(t) is described by a sum of exponentials

$$I(t) = \sum_j \frac{f_j}{(\tau_{dj} - \tau_{rj})} \left[e^{-(t-t_0)/\tau_{dj}} - e^{-(t-t_0)/\tau_{rj}} \right], \qquad (1)$$

where the integrated intensity is normalized to unity,

$$\int_0^\infty I(t)\,dt = \sum_j f_j = 1. \qquad (2)$$

The observed fluorescence decay intensity $H(t)$ is the intrinsic intensity $I(t)$ convolved with the impulse response function $G(t)$:

$$H(t) = \int_0^\infty I(t')G(t-t')dt. \qquad (3)$$

The number of events expected in the kth time bin for a particular sum of exponential components is given by

$$N_k = A \int_{t_k}^{t_{k+1}} [H(t) + B]\,dt\ , \qquad (4)$$

where A is a normalization factor defined so that the total number of measured events is equal to the total number of expected events:

$$\sum_k M_k = \sum_k N_k\ . \qquad (5)$$

This analysis allows for the unequal time bin width that results from our data compression method.

Chi-squared is defined in the usual manner and minimized using a robust version of the Powell's Quadratically Convergent Method [8]. The index k runs over the 1900 time bins.

$$\chi^2 = \sum_k \frac{(M_k - N_k)^2}{N_k} . \quad (6)$$

IV. Results

A. Accuracy of Fast Rise Times

Figure 5 shows the data and best fit curves for a 2 x 10 x 10 mm BaF_2 crystal painted black on five sides, using an x-ray tube response of 60 ps (determined in Figure 4) and rise times constrained to be 0 ps and 30 ps. The fit with 0 ps rise time is excellent and the fit using a 30 ps rise time is poor. Considering the uncertainty in the x-ray tube response and the possibility of delayed photons from light scattering even for small crystals painted black, we estimate that the uncertainty in our fitted rise times is 30 ps.

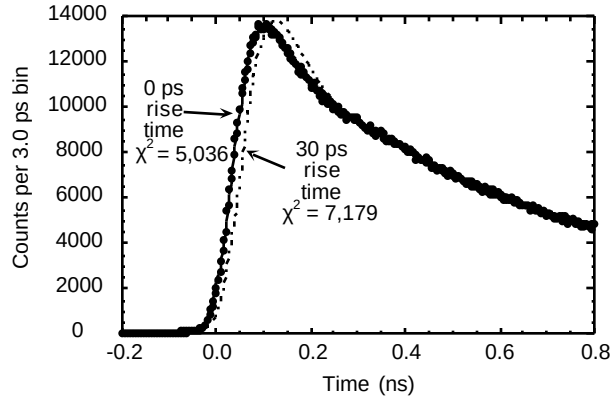

Figure 5: Data and best fit curves for a BaF_2 2 x 10 x 10 mm crystal painted black on 5 sides. See text for details.

B. Scintillator Rise Times

Figure 6 shows the $YAlO_3$:Ce time spectrum data with the best fit rise time of 240 ps. Figure 7 shows the $PbWO_4$ time spectrum data with the best fit rise time of 60 ps.

Figure 8 shows the CsI:Tl time spectrum data with the best fit rise time of 15 ns. A filter was used to block exciton emissions < 500 nm. The slow rise time is due to the thermal diffusion of relaxed holes and depends both on the initial concentration of charge carriers and on temperature [9].

Table 1 summarizes the best fit rise times for common scintillators. The shorter decay times are also listed.

V. Conclusions

The intrinsic and self activated scintillators CsI, $Bi_4Ge_3O_{12}$, CeF_3, and $CdWO_4$ have fast ($\leq$ 30 ps) rise times, indicating that the excited states are rapidly created after an ionization event. In these scintillators the luminescent centers have high concentrations and holes promptly form at or near these centers and then trap electrons to form the excited state. The activated scintillators Lu_2SiO_5:Ce, CaF_2:Eu, and ZnO:Ga have high luminosity and fast ($\leq$ 40 ps) rise times, indicating that holes are efficiently trapped by the low concentration activator atoms rather than by the crystal lattice. The activated scintillators $YAlO_3$:Ce and CsI:Tl have slower rise times due to processes that delay the transport of charge carriers to the activator atom.

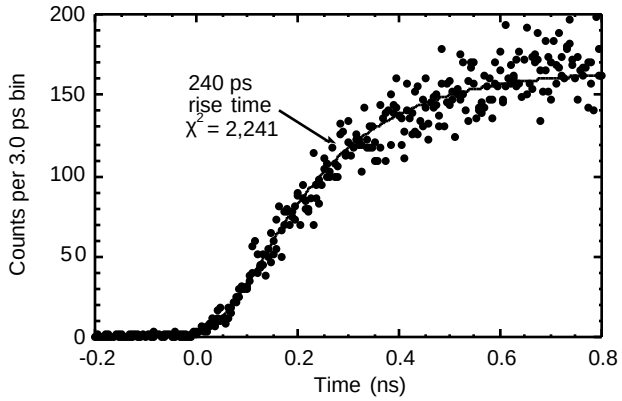

Figure 6: $YAlO_3$:Ce 10-mm cube painted black on five sides. Best fit rise time is 240 ps.

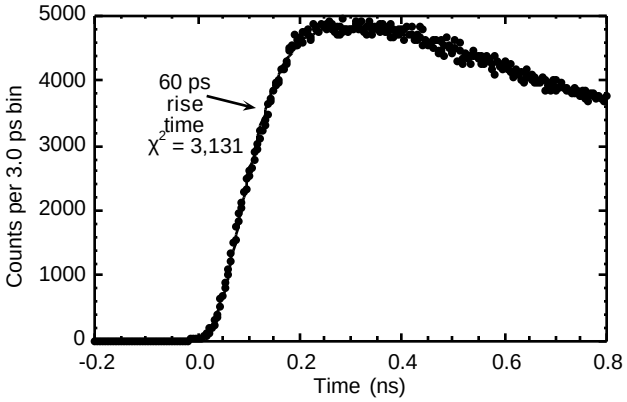

Figure 7: $PbWO_4$ 2 x 10 x 10-mm painted black on five sides. Best fit rise time is 60 ps.

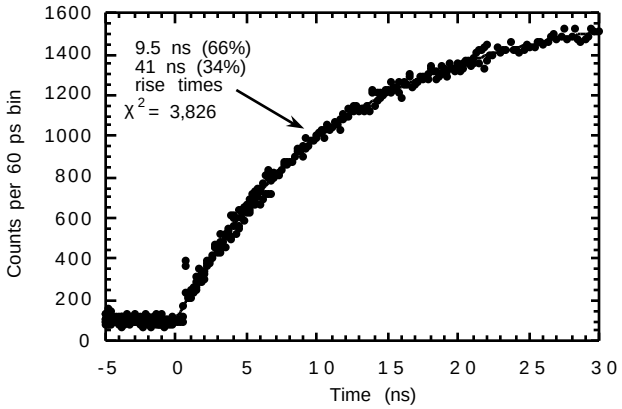

Figure 8: CsI:Tl 10-mm cube painted black on five sides. Fit requires two risetimes.

Table 1.
Description of samples measured and best fit rise times.

Sample	Form*	Supplier**	τ_r (ps)†	τ_d (ns)††
BaF_2	2 x 10 x 10 mm	Harshaw	0 (calibration)	0.12(2%), 0.78(12%) + longer
BaF_2	powder	Aesar, Inc.	< 30	0.18(2%), 0.88(8%) + longer
BC-422	2 x 10 x 20 mm	Bicron	< 30	1.1(59%), 2.3(29%) + longer
$Bi_4Ge_3O_{12}$	3 x 3 x 30 mm	Harshaw	30 ±30	5.8(1%), 28(4%) + longer
CaF_2:Eu	2 x 30 x 30 mm	Bicron	40±30	slow decay components
CeF_3	2 x 10 x 10 mm	Optovac	30 ±30	several decay components
CdS:Te	2 x 5 x 10 mm	Peter Trower	80 ±30	several decay components
$CdWO_4$	2 x 10 x 10 mm	Harshaw	< 30	13(1%) + longer
CsI	2 x 10 x 10 mm	Bicron	30±30	several decay components
CsI:Tl	10 x 10 x 10 mm	Optovac	9,500(66%), 41,000(34%)§	long decay
Lu_2SiO_5:Ce	3 x 3 x 30 mm	CTI	30 ±30 (88%), 350±70(12%)	7(1%), 38.8(99%)
$PbWO_4$	2 x 10 x 10 mm	FSU	60 ±30	several decay components
$YAlO_3$:Ce	10 x 10 x 10 mm	Peter Trower	240±50	26(90%), 67(10%),
ZnO:Ga	powder	Westinghouse	< 30	0.36(35%), 0.82(65%)

*All samples (except powders) roughened and painted black on five sides
**Bicron Chemical, Solon, Ohio; FSU = Former Soviet Union; CTI, Inc. Knoxville. TN; Optovac, Inc., North Brookfield, MA.
†Best fit rise time using x-ray tube calibration of 60 ps fwhm shown in Figure 4.
††Decay times may vary from sample to sample.
§Rise time is temperature dependent. See Ref. [9].

VI. Acknowledgments

We thank R. Deich for helpful discussions, D. Anderson and P. Trower for providing crystals, and M. Ho for technical assistance. This work was supported in part by the Director, Office of Science, Office of Biological and Environmental Research, Medical Science Division of the U.S. Department of Energy under Contract No. DE-AC03-76SF00098 and in part by Public Health Service grant number R01 CA48002 awarded by the National Cancer Institutes, Department of Health and Human Services. Reference to a company or product name does not imply approval or recommendation by the University of California or the U.S. Department of Energy to the exclusion of others that may be suitable.

VII. References

[1] S. E. Derenzo, W. W. Moses, S. C. Blankespoor, M. Ito, and K. Oba, "Design of a pulsed x-ray system for fluorescent lifetime measurements with a timing resolution of 109 ps," *IEEE Trans Nucl Sci*, vol. NS-41, pp. 629–631, 1994.

[2] S. C. Blankespoor, S. E. Derenzo, W. W. Moses, C. S. Rossington, M. Ito, and K. Oba, "Characterization of a pulsed X-ray source for fluorescent lifetime measurements," *IEEE Trans Nucl Sci*, vol. NS-41, pp. 698-702, 1994.

[3] S. C. Blankespoor, "Design and characterization of a pulsed x-ray source for fluorescent lifetime measurements (Masters Thesis) (LBL Report No. LBL-35092)," : University of California, Berkeley, 1993.

[4] L. M. Bollinger and G. E. Thomas, "Measurement of the time dependence of scintillation intensity by a delayed-coincidence method," *Rev Sci Instr*, vol. 32, pp. 1044-1050, 1961.

[5] C. Cottini, E. Gatti, and V. Svelto, "A new method for analog to digital conversion," *Nucl Instr Meth*, vol. 24, pp. 241-242, 1963.

[6] R. A. Lerche and D. W. Phillion, "Risetime of BC-422 plastic scintillator <20 ps," *IEEE Conference Record for the 1991 Nuclear Science Symposium, Santa Fe, NM*, pp. 167-170, 1991.

[7] W. Lehman, "Edge emission of n-type conducting ZnO and CdS," *Solid-State Electronics*, vol. 9, pp. 1107-1110, 1966.

[8] W. H. Press, B. P. Flannery, S. A. Teukolsky, and W. T. Vetterling, *Numerical Recipes in C*. Cambridge, England: Cambridge University Press, 1988.

[9] J. D. Valentine, W. W. Moses, S. E. Derenzo, D. K. Wehe, and G. F. Knoll, "Temperature dependence of CsI(Tl) gamma-ray scintillation decay time constants and emission spectrum," *Nucl Instr Meth*, vol. A325, pp. 147-157, 1993.